

Photon trapping and transfer with solitons

Ken Steiglitz^{1,*} and Darren Rand^{2,†}

¹*Department of Computer Science, Princeton University, Princeton, New Jersey 08544, USA*

²*Lincoln Laboratory, Massachusetts Institute of Technology, 244 Wood Street, Lexington, Massachusetts 02420, USA*

(Received 16 October 2008; published 12 February 2009)

We show, numerically, that a single photon trapped by a soliton in a Kerr nonlinear medium can be transferred from one soliton to another when the captor soliton undergoes collision with a second soliton. Soliton collisions can also be used in this way to realize a beam splitter, as well as a mode-separating beam splitter, analogous to the usual polarizing beam splitter. We discuss briefly the feasibility of an optical fiber implementation and possible applications to quantum-information processing.

DOI: [10.1103/PhysRevA.79.021802](https://doi.org/10.1103/PhysRevA.79.021802)

PACS number(s): 42.65.Tg, 42.50.Ex, 42.65.Jx, 42.79.Fm

An optical soliton in a homogeneous medium such as a fiber is characterized, ideally, by undistorted propagation and elastic collisions. It arises because of an intensity-dependent change in the fiber's refractive index. For a temporal soliton, this refractive index change creates a traveling potential, which can serve as a waveguide for another optical pulse (the *probe*). Similarly, a spatial soliton imprints a waveguide in the medium, an effect that has been confirmed in both Kerr [1] and photorefractive media [2–5]. In this Rapid Communication we show that when a soliton (the *pump*) collides with another soliton, the corresponding probe wave can be transferred almost perfectly from one soliton to another, or, depending on the conditions, split between two solitons, in perfect analogy to a beam splitter.

In the quantum limit where the probe wave represents a single photon, these effects may find application to the storage, transport, and routing of qubits. Its delivery by a soliton means that a single photon will be subject to reduced dispersion compared with unguided transmission; its arrival time will be known more precisely and timing jitter reduced. This may be beneficial in quantum-communication applications as bit rates and propagation distances increase. Beyond this, the proposed implementation of a mode-splitting beam splitter suggests application to quantum computing using linear optics [6]. Pittman *et al.* [7] show, in fact, that a polarizing beam splitter completely analogous to the mode-splitting beam splitter described here can be used to realize a controlled-NOT gate. Soliton-guided photons—in a fiber, for example—may thus provide a natural medium for optical quantum gate implementation.

Following Manassah [8,9], de la Fuente and Barthelemy [1], and Ostrovskaya *et al.* [10] we model the system of interest with two coupled wave equations, the first being a standard cubic nonlinear Schrödinger equation for the pump, and the second a linear wave equation for the probe signal, which is assumed to be very much weaker than the pump. Thus, the propagation of the pump signal $P(z, t)$ is governed by

$$i \frac{\partial P}{\partial z} + \gamma_p |P|^2 P - \frac{\beta_{2p}}{2} \frac{\partial^2 P}{\partial t^2} = 0, \quad (1)$$

where t is local time, z is propagation distance, β_{2p} represents the group velocity dispersion of the pump, and γ_p is a nonlinearity parameter. We neglect higher-order dispersion and assume a lossless medium with an instantaneous electronic response. We would like to use the exact two-soliton solution given in [11]. To this end we scale z by letting $x = -(\beta_{2p}/2)z$, which yields Eq. (2), and the pump $\hat{P}(x, t)$ in the notation of [11] with $\mu_p = -\gamma_p/\beta_{2p}$ (we will take $\beta_{2p} < 0$ and $\gamma_p > 0$, so $\mu_p > 0$):

$$i \frac{\partial \hat{P}}{\partial x} + 2\mu_p |\hat{P}|^2 \hat{P} + \frac{\partial^2 \hat{P}}{\partial t^2} = 0. \quad (2)$$

The general, ground-state, single-soliton solution of Eq. (2) is given by [11]

$$\hat{P}(x, t) = \frac{|k_R|}{\sqrt{\mu_p}} e^{i[k_I(t-t_0) + (k_R^2 - k_I^2)x]} \operatorname{sech}[k_R(t - t_0 - 2k_I x) + \phi], \quad (3)$$

where the free complex parameter $k = k_R + ik_I$, k_R determines the energy of the soliton, and k_I its velocity, all in normalized units. To launch the soliton along the $t=0$ axis, we choose $t_0 = \phi/k_R$ and the velocity $k_I=0$, so that the single-soliton solution is

$$\hat{P}(x, t) = \frac{|k_R|}{\sqrt{\mu_p}} e^{ik_R^2 x} \operatorname{sech}(k_R t). \quad (4)$$

The use of the closed-form two-soliton solution [11] ensures that the computation of the pump is both fast and accurate.

The linear equation for the propagation of the probe wave $u(z, t)$ is

$$i \left(\frac{\partial u}{\partial z} + (\beta_{1s} - \beta_{1p}) \frac{\partial u}{\partial t} \right) + \gamma_s |P|^2 u - \frac{\beta_{2s}}{2} \frac{\partial^2 u}{\partial t^2} = 0, \quad (5)$$

where $P(z, t)$ is the soliton pump and γ_s is a nonlinearity parameter. Here, $\beta_{1\{p,s\}} = 1/v_{g\{p,s\}}$, $v_{g\{p,s\}}$ is the group velocity of the pump and probe, β_{2s} is the group velocity dispersion of the probe, and the term in $(\beta_{1s} - \beta_{1p})$ represents the walkoff between the probe and pump. Taking the walkoff

*ken@cs.princeton.edu

†drand@ll.mit.edu

term to be zero and using the one-soliton solution in Eq. (4) as the soliton pump, the probe equation becomes

$$i\frac{\partial u}{\partial z} + \gamma_s \frac{k_R^2}{\mu_p} \operatorname{sech}^2(k_R t) u - \frac{\beta_{2s}}{2} \frac{\partial^2 u}{\partial t^2} = 0. \quad (6)$$

Notice that the intensity of the pump does not vary with propagation distance z . When we come to use the two-soliton solution of Eq. (2), however, the scaling of z will matter.

To reduce the probe equation to a z -independent eigenvalue problem, let

$$u(z, t) = u(t) e^{-iEz}, \quad (7)$$

yielding

$$\frac{\beta_{2s}}{2} u'' - \left(E + \gamma_s \frac{k_R^2}{\mu_p} \operatorname{sech}^2(k_R t) \right) u = 0. \quad (8)$$

We use the transformation [12]

$$\xi = \tanh(k_R t), \quad (9)$$

to put this equation in the form

$$\frac{d}{d\xi} \left((1 - \xi^2) \frac{du}{d\xi} \right) + \left(\ell(\ell + 1) - \frac{m^2}{(1 - \xi^2)} \right) u = 0, \quad (10)$$

where

$$m^2 = 2E / (k_R^2 \beta_{2s}) \quad (11)$$

and

$$\ell(\ell + 1) = -2\gamma_s / (\mu_p \beta_{2s}) = 2\mu_s / \mu_p, \quad (12)$$

where $\mu_s = -\gamma_s / \beta_{2s}$. This is the associated Legendre equation, with solutions (eigenfunctions) $u_{\ell m}$ of degree ℓ and order m that are nonsingular and physically acceptable for integers $\ell \geq m \geq 0$. Each $u_{\ell m}$ is the product of $(1 - \xi^2)^{m/2}$ and a polynomial in ξ of degree $(\ell - m)$ and parity $(-)^{\ell - m}$, with $(\ell - m)$ zeros in the interval $-1 \leq \xi \leq +1$ [13,14]. As functions of t the solutions of Eq. (10) take the form $\operatorname{sech}^m(k_R t)$ times a polynomial in $\tanh(k_R t)$ of degree $(\ell - m)$. (A convenient list of associated Legendre functions in explicit form is given in [15].) Note that the degree of the wave functions supported in the induced waveguide is determined solely by the ratio of the μ parameters between the probe and pump equations.

Restrict attention to the cases where ℓ and m are integers, when the system described by Eq. (10) supports analytically known eigenfunctions in the induced waveguide. We also exclude the cases where $\ell = 0$ or $m = 0$ because the corresponding solutions do not decay to zero at $t = \pm \infty$. Assume that we design the fixed physical parameters of the system, γ_s , β_{2s} , γ_p , and β_{2p} , to ensure that ℓ given by Eq. (12) is integer. [In simulations we choose γ_s , γ_p , β_{2p} , and ℓ , and then use Eq. (12) to determine β_{2s} . In general, such values may not be realizable in a fiber implementation.] Then there are exactly ℓ eigenfunctions supported by the induced waveguide, corresponding to $m = 1, \dots, \ell$. Equation (11) gives the corresponding energy eigenvalues E_1, \dots, E_ℓ . When more than one of these copropagate the difference in these energy levels causes beating in the z direction [see Eq. (7)], as dis-

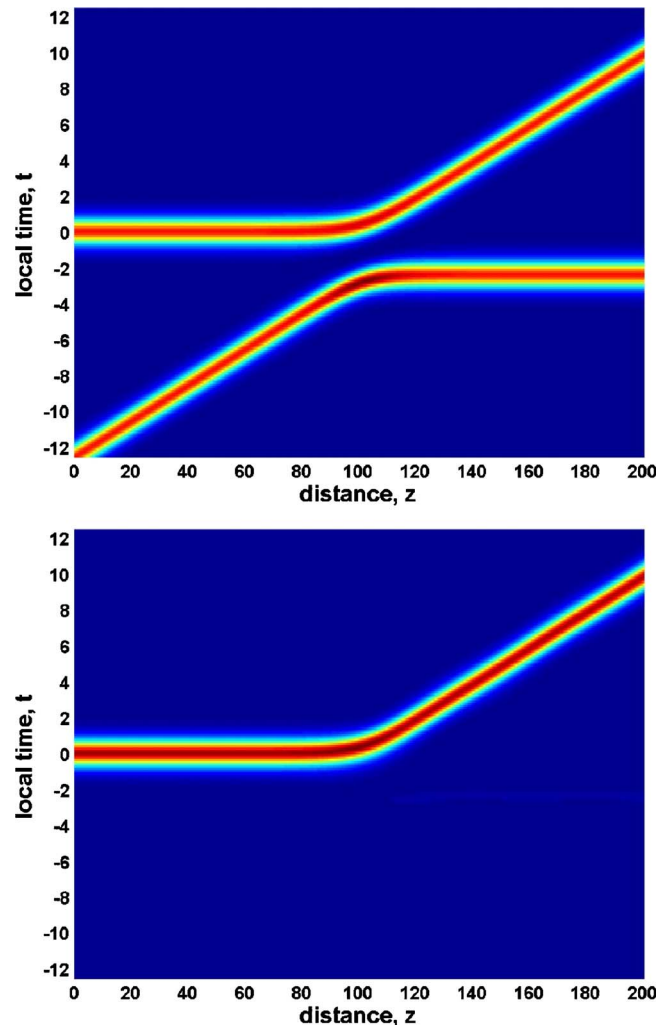


FIG. 1. (Color online) An example of photon transfer. Top: The pump solitons. The soliton parameters in the notation of [11] are $k_1 = 1.5$, $k_2 = -1.5 + 0.5i$, $\mu_p = 0.1$ ($\gamma_p = 0.02$, $\beta_{2p} = -0.2$), and the amplitudes of both (scalar) solitons are 4. The relative phase at collision is arranged to be π . Bottom: The probe when launched in the state |11). The parameters for the probe propagation are $\gamma_s = 0.01333$ and $\beta_{2s} = -0.1333$ ($\ell = 1$). The photon is transferred to the overtaking soliton.

cussed in [8]. From now on we think of the probe as a single photon in the weak-signal quantum limit, and start with the simplest case, when $\ell = m = 1$. This corresponds to the single-peaked ground state u_{11} , which we denote by |11).

We now consider something new: we launch a photon trapped by a soliton, soliton 1, and launch a second soliton after it, soliton 2, at greater speed, so that it overtakes soliton 1. In the z - t plane, soliton 1 is launched in the positive z direction, along the $t = 0$ line, say, and soliton 2 travels up and to the right so that it collides with soliton 1. What, then, happens to the photon originally trapped by soliton 1? Figure 1 (top) shows the pump solitons (from the exact analytical solution in [11]) in a typical example, and Fig. 1 (bottom) shows the corresponding resulting probe (from numerical integration): the photon is almost perfectly transferred from the first to the second soliton. The results shown for the probe were obtained by numerically integrating Eq. (5) using the

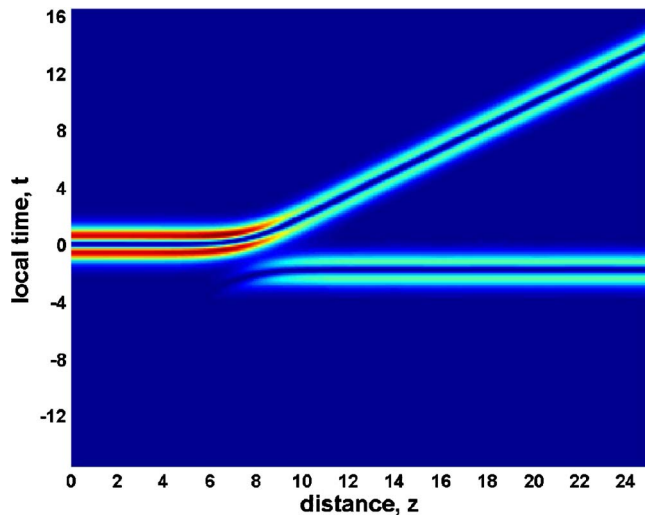


FIG. 2. (Color online) The probe when launched in the state $|21\rangle$. In this case $\gamma_s=4$ and $k_2=-1.5+0.8i$, so that the soliton collision takes place at a greater relative velocity. The system acts as an ordinary nonpolarizing beam splitter.

split-step Fourier method. The initial condition used for numerical integration is the analytical solution $u_{\ell m}$ of Eq. (10), and we again assume a zero walkoff term in Eq. (5). The extra velocity is imparted to the photon on transfer, not by a walkoff term, but by the moving potential which results from the two-soliton solution for the pump.

It is important to note that we have arranged things to make the relative phase of the solitons at collision exactly π , producing a so-called “repulsive” collision. This results in an effective waveguide that can be made to bend more or less gently, depending on the relative speed of the soliton collision. When the relative phase at collision is much different from π , the soliton collision no longer induces a smoothly bent waveguide, and the behavior becomes more complicated and remains to be explored.

The experimental demonstration of such photon trapping and transfer should be feasible with current optical fiber technology. As an example, we assume a scheme with perpendicularly polarized pump and probe in a polarization maintaining fiber where the birefringence has a standard off-the-shelf value of about 3×10^{-4} . We take soliton pulse widths on the order of 1 ps, wavelength separation between solitons of a few nanometers, and standard fiber parameters of dispersion and nonlinearity at a wavelength of 1550 nm. At this wavelength, losses are minimized, which is important for both single-photon and soliton propagation. In order to operate with no walkoff, we require about 50 nm wavelength separation between pump and probe to compensate for birefringence-induced walkoff [16]. These operating parameters should allow for propagation and collision experiments to occur within about 1 or 2 km of fiber, and this wavelength separation should make possible the detection of single photons in the probe. The physical parameters of Fig. 1 were chosen to agree with this particular implementation.

The model of photon transfer described above assumes perpendicular polarization in a birefringent fiber with realistic parameter values and a mode of first degree, $\ell=1$. If we

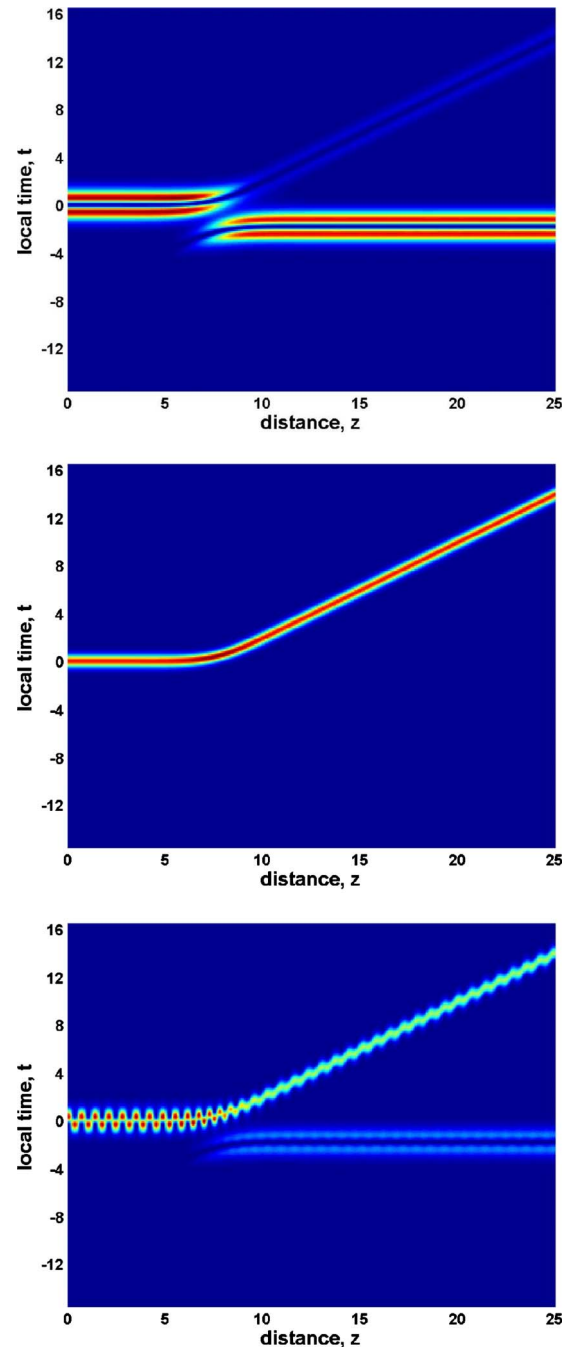


FIG. 3. (Color online) Top: The probe when launched in the excited state $|21\rangle$, with the same parameters as for Fig. 2, except $\gamma_s=8$. The photon in this case stays in large part with its original captor soliton. Center: The probe when launched in the state $|22\rangle$. The photon is transferred to the faster soliton, as in the $|11\rangle$ case shown in Fig. 1. Bottom: The probe when an equal linear combination of ground and excited states, $|22\rangle+|21\rangle$, is launched. The system is analogous to a polarizing beam splitter.

can realize other, higher values of γ_s , by moving away from fiber optic implementation, we can observe a further wide range of interesting phenomena. Consider, for example, the case with the same basic collision geometry, but where we take $\gamma_s=4$, increase the relative velocity of the collision by taking $k_7=0.8$, and launch the probe in the state $|21\rangle$.

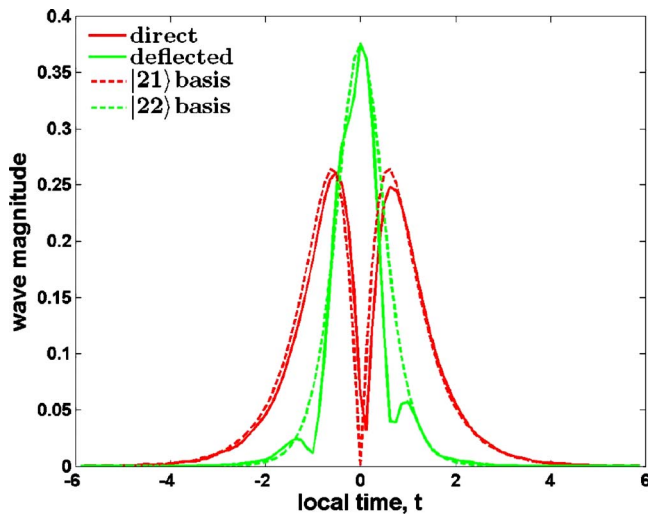


FIG. 4. (Color online) Probe waveform profiles for the linear combination case shown in Fig. 3 (bottom).

Figure 2 shows the somewhat surprising result: the probe wave is transmitted and deflected in about equal measure (with a relative phase of π). In other words, the system acts as an ordinary (nonpolarizing) beam splitter.

For the final example, we use the same parameters as for the non-polarizing beam splitter, except we increase γ_s to 8. Figure 3 (top) shows that now the state $|21\rangle$ is almost entirely transmitted. In contrast, Fig. 3 (center) shows that the ground state $|22\rangle$ is almost entirely deflected (the photon deflected), as was the ground state $|11\rangle$ in our first example.

The probe equation is linear, and this observation shows that this system is perfectly analogous to a polarizing beam splitter (PBS), except that the orthogonal modes separated are $|22\rangle$ and $|21\rangle$, instead of horizontal and vertical. When a linear combination of modes is launched with soliton 1, the excited-state component is largely transmitted directly, while the ground state is deflected. Figure 3 (bottom) shows the result when such a probe is launched, and Fig. 4 shows profiles of the magnitudes of the deflected and direct waves in their local axes (orthogonal to the direction of propagation),

together with the corresponding basis functions.

The efficiency of the PBS can be measured quantitatively by expanding the direct and deflected waves in terms of the orthonormal basis. The resultant projections squared, $|\langle u | u_{\ell m} \rangle|^2$, for the linear combination case in Figs. 3 (bottom) and 4 are

	Excited	Ground
Direct	0.926730	0.001626
Deflected	0.134425	0.732341

The rows represent the outputs and the columns the inputs. An ideal PBS would, of course, correspond here to an identity matrix.

We should point out that the parameters for the examples presented in this Rapid Communication have not by any means been exhaustively explored. The space of parameters is in fact quite large. There are the complex soliton parameters k_1 and k_2 , which determine the solitons' amplitudes (which need not be equal) and speeds; the relative soliton phase at collision; and the pump physical parameters γ_p and β_{2p} . The probe has its own physical parameters γ_s and β_{2s} (which then determine the degree ℓ), and the order m . Only a tiny fraction of this space has been touched. Nor have the possibilities for implementation of the beam splitters using current technology been explored, and work continues on the properties of soliton-guided photons in general. It may also be of interest to study the mechanism of differential transfer exhibited in the beam-splitter examples, which is reminiscent of quantum tunneling and frustrated total internal reflection.

In conclusion, we have shown that, when photons are trapped by solitons, soliton collisions can be used to implement several operations that may prove useful in quantum communication and computing: the trapping and transfer of qubits, a beam splitter, and a polarizing beam splitter. The transfer of qubits is practical in an optical fiber with today's technology.

D. R. was sponsored by the U. S. Department of the Air Force under Air Force Contract No. FA8721-05-C-0002.

- [1] Raül de la Fuente and Alain Barthelemy, *IEEE J. Quantum Electron.* **28**, 547 (1992).
- [2] M. Morin, G. Duree, G. Salamo, and M. Segev, *Opt. Lett.* **20**, 2066 (1995).
- [3] M.-F. Shih, M. Segev, and G. J. Salamo, *Opt. Lett.* **21**, 931 (1996).
- [4] M.-F. Shih, Z. Chen, M. Mitchell, M. Segev, H. Lee, R. S. Feigelson, and J. P. Wilde, *J. Opt. Soc. Am. B* **14**, 3091 (1997).
- [5] S. Lan, E. DelRe, Z. Chen, M.-F. Shih, and M. Segev, *Opt. Lett.* **24**, 475 (1999).
- [6] E. Knill, R. Laflamme, and G. Milburn, *Nature (London)* **409**, 46 (2001).
- [7] T. B. Pittman, B. C. Jacobs, and J. D. Franson, *Phys. Rev. A* **64**, 062311 (2001).
- [8] J. T. Manassah, *Opt. Lett.* **15**, 670 (1990).
- [9] J. T. Manassah, *Opt. Lett.* **16**, 587 (1991).
- [10] E. A. Ostrovskaya, Y. S. Kivshar, D. Mihalache, and L.-C. Crasovan, *IEEE J. Sel. Top. Quantum Electron.* **8**, 591 (2002).
- [11] R. Radhakrishnan, M. Lakshmanan, and J. Hietarinta, *Phys. Rev. E* **56**, 2213 (1997).
- [12] L. D. Landau and E. M. Lifshitz, *Quantum Mechanics: Non-Relativistic Theory*, 3rd ed. (Pergamon Press, Oxford, 1991).
- [13] A. Messiah, *Quantum Mechanics*, 1st ed. (North-Holland, Amsterdam, 1970).
- [14] L. I. Schiff, *Quantum Mechanics*, 3rd ed. (McGraw-Hill, New York, 1968).
- [15] E. J. Garboczi, *Cem. Concr. Res.* **32**, 1621 (2002).
- [16] K. S. Abedin, *Opt. Lett.* **30**, 2979 (2005).